

H-OWAN: Multi-distorted Image Restoration with Tensor 1×1 Convolution

Zihao Huang^{1,2}, Chao Li^{*2}, Feng Duan¹ and Qibin Zhao^{†2}

¹College of Artificial intelligence, Nankai University, Tianjin, China

²Riken Center for Advanced Intelligence Project, Tokyo, Japan

Abstract

It is a challenging task to restore images from their variants with combined distortions. In the existing works, a promising strategy is to apply parallel “operations” to handle different types of distortion. However, in the feature fusion phase, a small number of operations would dominate the restoration result due to the features’ heterogeneity by different operations. To this end, we introduce the tensor 1×1 convolutional layer by imposing high-order tensor (outer) product, by which we not only harmonize the heterogeneous features but also take additional non-linearity into account. To avoid the unacceptable kernel size resulted from the tensor product, we construct the kernels with tensor network decomposition, which is able to convert the exponential growth of the dimension to linear growth. Armed with the new layer, we propose High-order OWAN for multi-distorted image restoration. In the numerical experiments, the proposed net outperforms the previous state-of-the-art and shows promising performance even in more difficult tasks.

1 Introduction

Image restoration (IR), the operation of taking a corrupt image and reconstructing its clean counterpart, is a fundamental task in computer vision. At present, deep-learning-based methods have shown remarkable success in this task particularly when images are corrupted by a specialized type of distortion (*e.g.*, Gaussian noise [19], Gaussian blur [20]). However, in practical applications like autopilot vision and surveillance, the distortion would be a mixture of various types with unknown strength. It therefore degrades the performance of methods in the real world.

There are recently several methods proposed to tackle this issue [18, 21, 22]. A common idea in these methods is to construct a deep network with multiple “operational layers/sub-nets”, of which different types are expected to deal with different distortion. For example, a reinforcement-learning

*Equal contribution with the first author.

†Corresponding author. Email: {chao.li, qibin.zhao}@riken.jp

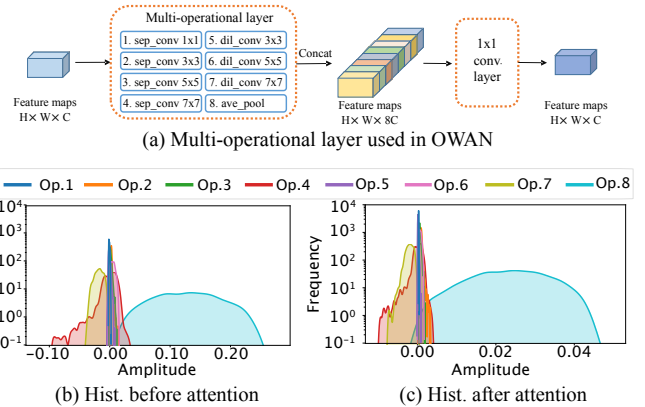


Figure 1: Multi-operational layers used in OWAN (a) and the estimated distribution of the feature maps by each operation. In Panel (a), the keywords “sep_conv” and “dil_conv” denotes the separable and dilated convolutional layer with specified size, respectively. Panel (b) and (c) shows the histogram of the feature maps by eight operations in the test phase, where (b) and (c) corresponds the results before and after the attention module. More details are given in Sec. 2.

agent is trained in [22] for automatically selecting suitable operations. Operation-wise attention network (OWAN) [18], as the state-of-the-art (SOTA) approach so far, simultaneously performs eight different operations on feature map following an 1×1 convolutional layer (see Figure 1 (a)). Although these methods outperform the previous approaches on the multi-distorted IR task, a critical issue is generally omitted in existing methods: *The parallel network architecture with different “operations” would lead to heterogeneous feature maps.* Figure 1 (b) and (c) show the histogram of the feature maps by different operations in OWAN (see Section 2 for details). We will show that some operations would consequently dominate the restoration results due to the heterogeneity.

To this end, we propose a novel tensor 1×1 convolutional layer (T1CL), by which we can effectively alleviate the aforementioned issue and as the result significantly improve the restoration quality. Compared to the conventional 1×1 convolutional layer, the new layer extends the linear operations into multi-linear forms, where for each pixel a tensor kernel is repeatedly multiplied (*i.e.* tensor-product) by the features

along every “direction” (see Figure 3). Due to the multi-linearity, the entanglement among channels is enhanced. In the context of the networks like OWAN, concatenating the feature maps by multiple operations along the channel direction, the stronger entanglement is able to harmonize the heterogeneous features and consequently improve the restoration performance. More interestingly, the experimental results illustrate that the imposed multi-linearity also has the capacity to improve the representation power of the network. It implies that the networks equipped with the new layers would achieve promising performance in more challenging tasks.

In Section 2, we discuss the feature heterogeneity and the domination issue in detail by focusing on OWAN. The notion of tensor 1×1 convolution layer is introduced in Section 3, where we also show *tensor network decomposition* [13, 25] can efficiently reduce the exponentially-increasing dimension of the tensor kernel.

In the experiment, we equip the proposed layer into OWAN by replacing the conventional 1×1 convolutional layers. Armed with the new layer, the high-order form of OWAN (*a.k.a.* H-OWAN) outperforms the previous SOTA approaches on the multi-distorted IR task. Further, the experimental results show that the performance improvement is kept under various hyper-parameters and models. Last, H-OWAN also shows promising performance in a more challenging task, where more types of distortion are concerned in the experiment.

1.1 Related Work

Image restoration Given a specialized type of distortion, at present, the state-of-the-art performance is generally achieved by approaches with deep convolutional neural networks (CNNs) [5, 8, 14, 16, 19, 20] to name a few. On the other hand, there is few studies focusing on the IR task with combined distortion under unknown strength, *i.e.* multi-distorted image restoration. In a relatively early stage, “DnCNN” [24], a residual-CNN inspired method, was proposed to deal with blind Gaussian denoising problem. More recently, [21] tackle the multi-distorted IR task using “RL-Restore”, which learn a policy to select appropriate networks from a “toolbox”. Also using reinforcement learning, “Path-Restore” [22] is able to adaptively select an appropriate combination of operations to handle various distortion. Apart from the methods above, [18] proposed “OWAN”, a deep CNN with multi-operational layer and attention mechanism, which achieved the state-of-the-art performance on the multi-distorted IR task. In contrast to developing novel architectures, in this paper we focus on the heterogeneity and domination issue of feature maps due to the parallel structure of operations/subnets (especially in OWAN). We argue that such heterogeneity would degenerate the performance, but this issue can be alleviated by the proposed tensor 1×1 convolutional layer.

Feature fusion with tensor product Tensor (or outer) prod-

uct is popularly used in deep learning for feature fusion, and achieves promising performance in various applications. One line of work is to fuse the features from multi-modal data like visual question answering (VQA) [1] or sentiment analysis [10]. In these methods, different feature vectors will multiply tensor weights along different directions. Another line of the work is generally called polynomial/high-order/exponential trick [3, 12, 23]. In contrast to the cases in multi-modal learning, the tensor weights are generally symmetric and will be repeatedly multiplied by the same feature vector. Furthermore, in both two lines, tensor decomposition is generally used for dimension reduction. The proposed layer in this paper is inspired by the second line of this work. The difference is that the focus of our work is on the heterogeneity issue rather than multi-modal feature fusion. Furthermore, to our best knowledge, it is the first time to apply this higher-order structure to the extension of convolutional layers.

2 Features’ Heterogeneity in OWAN

Below, we focus on the OWAN method to discuss how multiple operations lead to heterogeneous feature maps and show that part of the operations would dominate the restoration results in the interference phase.

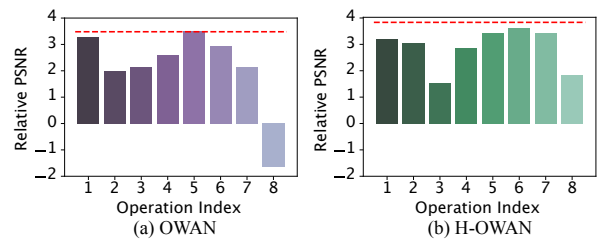


Figure 2: Relative PSNR of the test set when removing one operation. Relative PSNR is the difference with a benchmark, which is the PSNR of the distorted images. The red line of dashes means the performance of maintaining all operational layers.

Recall the multi-operational layer used in OWAN ¹. As shown in Figure 1, the feature maps are filtered by eight different operations in parallel. The filtered features are subsequently concatenated and go through a 1×1 convolutional layer. To verify the features’ heterogeneity from different operations, we set up the following illustrative experiments: For simplicity, we squeeze the scale of OWAN with only 4 multi-operational layers and use randomly selected 5000 and 3584 patches from the dataset for training and testing, respectively. In the training phase, Adam optimizer is applied until 100 epochs such that the network converges completely. Panel (b) and (c) in Figure 1 shows the estimated distribution of the features *w.r.t.* each operation of the 4th multi-operational

¹Here we omit the corresponding attention path for brevity.

layer in the inference phase, where the two panels (b) and (c) correspond the results before and after the attention operation, respectively. We can see that the distributions are significantly different from each operation: Most of them are quite close to zero, while some are spread in a wide range of values.

The reason resulting in this issue is due to the very different structures of the operations. For example, Op. 8 represents the average pooling layer, of which the output value is naturally larger than ones by convolutional layers with small weights. Compared between the two plots, the attention module seems to be able to relatively weaken the heterogeneity, but the effect is only on the scale and might not be significant.

Next, we show how much contribution is made by each operation on the restoration task. To do so, we evaluate the peak relative signal-to-noise ratio (PSNR) of the restored test samples under the condition that we “close” the outputs of each operation in turn by setting them to equal 0. Figure 2 (a) shows the experimental results, where the red dashed line represents the performance without closing any operation. As shown in Figure 2 (a), the performance is significantly decreased when Op. 8 is closed, while the output by Op. 5 have almost no influence on the performance. It implies that in OWAN the contribution by different operations is unbalanced. Some of the operations like Op. 2 and 8 dominate the restoration results, while some of them like Op. 1 and 5 have little contribution. Such fact goes against the expectation that the multiple operations play their own to handle various types of distortion.

Can batch-normalization solve this issue? One may argue that the heterogeneity could be removed by imposing batch-normalization (BN) layer for each operation. Note by lots of studies that the restoration quality would be decreased when incorporating BN layers in the network [7, 15]. It is because BN would lead to the interaction of the restored images in the same batch. Furthermore, BN can only normalize the 1st and 2nd-order statistical characteristic of the features, and the higher-order characteristics are still out of control.

3 Tensor 1×1 Convolutional Layer

In this section, we first mathematically analyze the reason leading to the domination issue. After that, to address this issue, we propose an extension of the 1×1 convolutional layer by imposing p th-order tensor product, and further introduce how to exploit tensor network decomposition [13, 25] to reduce the unacceptable size of tensor kernels.

Notation For brevity of the formulas, we apply the Einstein notation to describe tensor-vector and tensor-tensor multiplication below [6]. For example, assume x_i and W_{ij} to denote a vector and 2rd-order tensor (*a.k.a.* matrix), respectively, then their product can be simply written as $y_j = W_{ij}x_i$. Given two

vectors $x_i^{(1)}, x_i^{(2)} \in \mathbb{R}^C$, we define the concatenation of two vectors as $x_i^{(1) \frown (2)} \in \mathbb{R}^{2C}$. In more general case, the concatenation of N vectors can be simply denoted by $x_i^{(1) \frown (N)}$ without ambiguity. Given a vector $x_i \in \mathbb{R}^C$, the p th-order tensor product of x_i is denoted by $(x_i^p)_{i_1, \dots, i_p} \in \mathbb{R}^{C^p}$.

Convolution with heterogeneous input Assume that we have totally N operations, and given a pixel let $x_i^{(1)}, x_i^{(2)}, \dots, x_i^{(N)}$ denote the output feature vectors for each operation, respectively. Since in OWAN these outputs are concatenated and subsequently go through a 1×1 convolutional layer (refer to Figure 1 (a)), the corresponding feature on the output side can be formulized as

$$y_j = \phi \left(W_{ij} x_i^{(1) \frown (N)} \right) = \phi \left(W_{ij}^{(1)} x_i^{(1)} + \underbrace{\dots + W_{ij}^{(k)} x_i^{(k)} + \dots}_{k\text{th-op.}} + W_{ij}^{(N)} x_i^{(N)} \right), \quad (1)$$

where $\phi(\cdot)$ denotes the activation function, y_j denotes the output feature vector given a pixel, and W_{ij} and $W_{ij}^{(n)}$, $n \in [N]$ represent the kernel and its partitions *w.r.t.* $x_i^{(n)}$, respectively. As shown in Equation (1), the feature y_j can be “decomposed” as a sum of components following a non-linear function ϕ , and we can see each component corresponds to different operations. It implies that one operation only affects one component in Equation (1). It naturally results in the fact that the value of y_i would be dominated if there exist components with a wide range of values (like Op. 4 and 8 in Figure 1), while the components concentrating to zero (like Op. 3 in Figure 1) will hardly affect the value of y_j . Hence, we claim that the inherent structure of 1×1 convolutional layer determines the aforementioned domination phenomena.

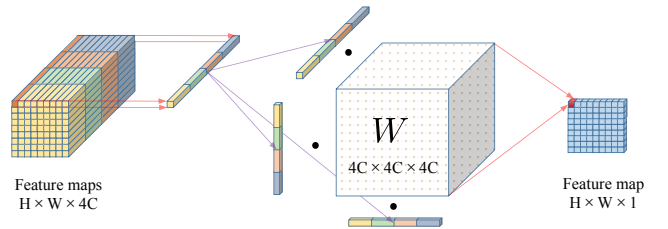


Figure 3: Illustration to the 3th-order tensor 1×1 convolution, in which the dimension of output channel equals 1.

Convolution via p th-order tensor product To address this issue, a natural idea is to construct a new form to fuse the features from multiple operations, of which the features can affect as many components in convolution as possible. Motivated by this, we extend the conventional 1×1 convolutional layer by imposing p th-order tensor product over the feature map.

Specifically, we extend Equation (1) into a p th-order version:

$$y_j = \phi \left(W_{i_1, \dots, i_p, j} \left(x^{(1) \wedge (N), p} \right)_{i_1, \dots, i_p} \right) \\ = \phi \left(\underbrace{W_{i_1, \dots, i_p, j} \cdot x_{i_1}^{(1) \wedge (N)} \cdot x_{i_2}^{(1) \wedge (N)} \cdot \dots \cdot x_{i_p}^{(1) \wedge (N)}}_{\text{tensor-vec. prod.}} \right). \quad (2)$$

We can see that the tensor kernel $W_{i_1, \dots, i_p, j}$ is repeatedly multiplied by the same input feature $x_{i_n}^{(1) \wedge (N)}$ along N directions. Figure 3 shows an example of the tensor 1×1 convolution when $p = 3$ and $j = 1$. As shown in Figure 3, the kernel is extended into a higher-order tensor compared to the conventional 1×1 convolutional layer. Also the imposing tensor-product converts the conventional linear convolution into a non/(multi)-linear form. The conventional 1×1 convolutional layer is a special case of the proposed tensor layer when $p = 1$.

Next, we show how the tensor 1×1 convolutional layer solve the aforementioned domination problem. As an illustrative example, we assume that only 2 operations are concerned and the order of layer $p = 2$. Like Equation (1), we can also “decompose” Equation (2) as

$$y_j = \phi \left(W_{i_1 i_2 j} \cdot x_{i_1}^{(1) \wedge (2)} \cdot x_{i_2}^{(1) \wedge (2)} \right) \\ = \phi \left(\begin{aligned} &W_{i_1 i_2 j}^{(1,1)} \cdot x_{i_1}^{(1)} \cdot x_{i_2}^{(1)} + W_{i_1 i_2 j}^{(1,2)} \cdot x_{i_1}^{(1)} \cdot x_{i_2}^{(2)} \\ &+ W_{i_1 i_2 j}^{(2,1)} \cdot x_{i_1}^{(2)} \cdot x_{i_2}^{(1)} + W_{i_1 i_2 j}^{(2,2)} \cdot x_{i_1}^{(2)} \cdot x_{i_2}^{(2)} \end{aligned} \right). \quad (3)$$

An graphical illustration of this equation is shown in Figure 4. We can see that the tensor product results in more entanglement among different operations. It implies that, with increasing the order p , the feature vector associated with a given operation would affect more components compared to Equation (1). Such entanglement of operations would balance the contribution of the features even though there is a heterogeneous structure among them.

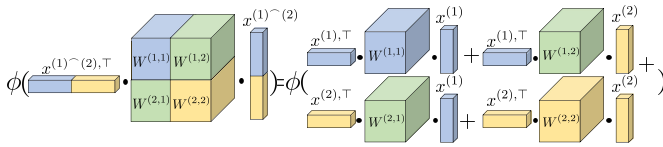


Figure 4: Illustration to Equation (3) with “decomposition” w.r.t. operations.

To validate this claim, we re-implement the experiment in Section 2 except replacing the conventional 1×1 convolutional layers by the proposed tensor form with $p = 2$. The experimental results are shown in Figure 2 (b). Compared to the results in Figure 2 (a), we can see that the influence on

the restoration quality by each operation is significantly alleviated.

Dimension reduction by tensor network decomposition

A critical issue brought from the new layer is that the kernel size will exponentially increased with the order p . To solve this problem, we apply *tensor network (TN)* decomposition to reduce the dimension of the kernel. TN decomposition is to represent a high-order tensor by a collection of smaller core tensors [17]. In this paper, we consider three popular types of TN decomposition models including canonical/polyadic (CP) [6], tensor-train (TT) [13] and TR [25]. Using the three models, the kernel in a p th-order tensor 1×1 convolutional layer can be represented by

$$W_{i_1, \dots, i_p, j}^{CP} = G_{i_1, r, j}^{(1)} G_{i_2, r, j}^{(2)} \dots G_{i_p, r, j}^{(p)}, \quad (4\text{-CP})$$

$$W_{i_1, \dots, i_p, j}^{TT} = G_{i_1, r_1, j}^{(1)} \dots G_{i_1, r_{k-1}, r_k, j}^{(k)} \dots G_{i_1, r_{p-1}, j}^{(p)}, \quad (4\text{-TT})$$

and

$$W_{i_1, \dots, i_p, j}^{TR} = G_{i_1, r_0, r_1, j}^{(1)} \dots G_{i_1, r_{k-1}, r_k, j}^{(k)} \dots G_{i_1, r_{p-1}, r_0, j}^{(p)}, \quad (4\text{-TR})$$

respectively. In the equations, the internal indices $r_k, \forall k$ is usually called bound dimension in physics literature [2] or *rank* in computer science [10], which controls the total number of parameters used in the layer. Since in layers the tensor kernel is multiplied by the same vector along all but the channel directions. Hence it is naturally to further assume the symmetric structure of the kernel, e.g., $G_{i_k, r, j}^{(k)} = G_{i_l, r, j}^{(l)}$ $k \neq l$ for the CP decomposition or $G_{i_k, r_{k-1}, r_k, j}^{(k)} = G_{i_l, r_{l-1}, r_l, j}^{(l)}$ $k \neq l$ for TR.

Complexity analysis Assume that the dimension of the input and output feature vectors to be equal to I and J , respectively. In this case, for each sample both the computational and storage complexity of the conventional 1×1 convolutional layer equals $\mathcal{O}(IJ)$ per pixel, while it increases to $\mathcal{O}(I^p J)$ for the vanilla p th-order form. If the kernel is represented by TN decomposition, the complexity can be decreased to $\mathcal{O}(pRIJ)$ for rank- R CP, and computationally $\mathcal{O}(p(R^2 I + R^3)J)$ and storely $\mathcal{O}(pR^2 IJ)$ for both TT and TR models with rank- R . We can see that TN decomposition successfully convert the complexity from exponential growth to a linear growth associated with the order p . In practice, the value of rank R is generally small, thus TN decomposition can significantly reduce the computational and storage requirement to implement the new layer.

4 Experiments

Below, we design three sets of experiments each addressing a different research question:

Test set	Mild (unseen)		Moderate		Severe (unseen)	
Metric	PSNR	SSIM	PSNR	SSIM	PSNR	SSIM
DnCNN	27.51	0.7315	26.50	0.6650	25.26	0.5974
RL-Restore	28.04	0.7313	26.45	0.6557	25.20	0.5915
Path-Restore	N/A	N/A	26.48	0.6667	N/A	N/A
OWAN	28.33	0.7455	27.07	0.6787	25.88	0.6167
H-OWAN-order2 (ours)	28.39	0.7485	27.13	0.6820	26.03	0.6207
H-OWAN-order3(ours)	28.35	0.7464	27.07	0.6810	25.99	0.6210
H-OWAN-order4(ours)	28.32	0.7430	27.06	0.6791	25.92	0.6176
H-OWAN-order2-add1(ours)	28.40	0.7474	27.10	0.6811	25.96	0.6183
H-OWAN-order3-add1(ours)	28.43	0.7479	27.11	0.6814	26.00	0.6187
H-OWAN-order4-add1(ours)	28.38	0.7473	27.13	0.6809	26.00	0.6185

Table 1: **Results on DIV2K.** Comparison of DnCNN, RL-Restore, Path-Restore, OWAN and our models using DIV2K test set. “order/*N*” denotes the order of the proposed T1CL, and “add1” means concatenating the feature map with a constant of 1 at the end. “N/A” means no results published.

E1: Armed with the tensor 1×1 convolutional layers (T1CLs), we compare the modified OWAN (high-order OWAN, H-OWAN) with previous state-of-the-art (SOTA) approaches in multi-distorted image restoration.

E2: We study the impact of the hyper-parameters imposed by the new layer like order and rank.

E3: We explore whether higher-order layers perform better on more difficult multi-distorted image restoration tasks.

4.1 E1: Comparison with SOTAs

Network setup To demonstrate the effectiveness of the proposed layer, we follow the same network setup to OWAN except that the used 1×1 convolutional layers are replaced by the new layers. The details of H-OWAN are as follows: we set up the network with 10 OWAN blocks [18], each of which contains 4 proposed T1CLs. For each T1CL, we apply the rank-16 CP decomposition to dimension reduction with the symmetric structures, *i.e.* shared core tensors. In the training phase, we apply the batch-averaged l_1 -distance between the restored images and its groundtruth as the loss function, and Adam optimizer [4] to training where $\alpha = 0.001$, $\beta_1 = 0.9$, and $\beta_2 = 0.99$. The initial learning rate equals 0.001 and the cosine annealing technique [11] is employed for adjusting. And our network is trained by 100 epochs with mini-batch size equaling 32.

DIV2K Dataset We evaluate the performance of our network by DIV2K dataset, which is also used in [18,21,22]. In the experiment, 800 images from DIV2K are selected and divided into two parts: 750 images as the training set and 50 images as the testing set. In addition, we clip each image into many 63×63 patches, where we totally have 230,080 and 3,584 patches in the training and test set, respectively.

Three types of distortion are considered in the experiment including Gaussian noise, Gaussian blur, and JPEG compression. They are mixed and added to the data with a wide range of degradation levels, which are separated into three groups: mild, moderate, and severe levels. To simulate the situation of unknown distortion strength, we only employ the moderate level on training data, but the testing data is generated at all three levels.

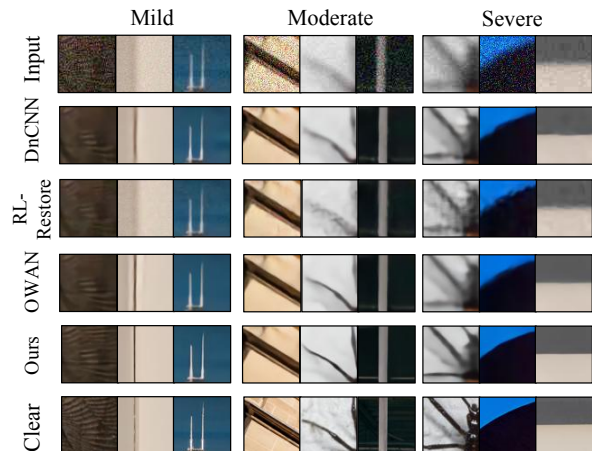


Figure 5: Examples of restored images by our method (H-OWAN-2order), OWAN, RL-Restore, and DnCNN.

Experimental results We compare the performance of H-OWAN with the SOTAs including DnCNN [24], RL-Restore [21], Path-Restore [22], OWAN [18]. The experimental results are shown in Table 1, where we implement H-OWAN with different orders and also consider the cases that incorporate a bias at the end of the feature map before the tensor product [6]. As shown in Table 1, H-OWAN under all conditions outperforms the previous SOTA approaches, and the best results are generally obtained when the order equals

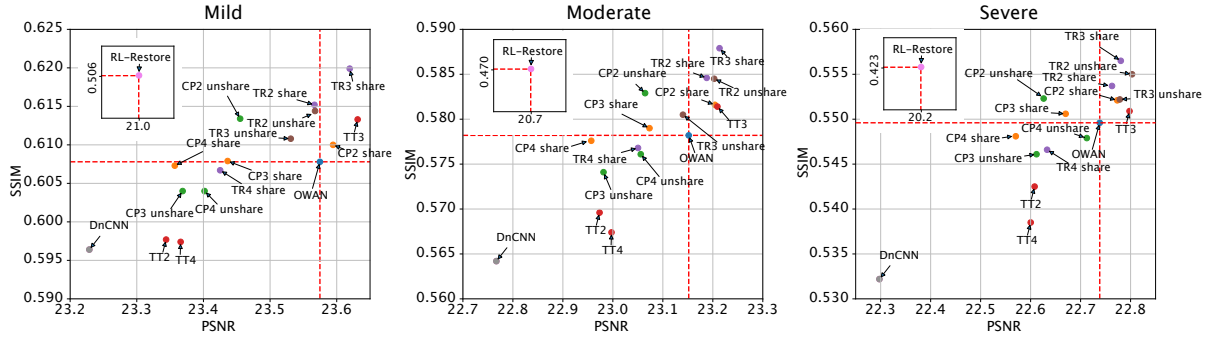


Figure 6: PSNR and SSIM results for image restoration with 5 types of distortion with different orders and tensor network decompositions in H-OWAN, where the number of blocks is set as 10.

2. Furthermore, imposing additional bias has no significant performance improvement in this experiment.

VOC	Method	mAP	VOC	Method	mAP
2007	w/o Restore	33.8	2012	w/o Restore	32.0
	OWAN	51.0		OWAN	51.2
	Ours	52.3		Ours	52.4

Table 2: **Results on PASCAL VOC.** Comparison of OWAN and our HOWAN-order2. A pretrained SSD300 is applied on distorted images ("w/o" Restore) and their restored versions.

Subsequent objective detection The image restoration task is generally employed as a pre-processing module following higher-level computer vision tasks. we therefore further evaluate the restoration performance by a subsequent object detection (OD) task, where we use the classic SSD300 [9] and corrupted/restored the PASCAL VOC test set in the experiment. Table 2 shows the mAP results where "w/o Restore" denotes "without restoration", and Figure 7 gives several illustrative examples of the experimental results. The results can demonstrate the effectiveness of H-OWAN.



Figure 7: Examples of object detection results on PASCAL VOC, where the color of boxes indicate class categories.

4.2 E2: Ablation Study on Hyperparameters

In this experiment, we evaluate the impact of the additional hyperparameters by T1CLs. In addition, we also concern whether the performance of the network equipped with T1CLs can be improved with increasing the depth of the network. Figure 8 shows the experimental results with all distortion level by (H-)OWAN under various orders, ranks and the number of OWAN blocks. As shown in Figure 8 (a), H-OWAN outperforms OWAN under all possible number of blocks and orders. With increasing the number of blocks, the restoration performance also gradually improves. However, the performance unexpectedly degenerates with increasing the order. We infer the reason for such results is because the representation power of order equaling 2 is sufficient for the current task, and higher order would lead to the training difficulty. The results in the next experiment will show that H-OWAN with higher orders has more promising performance on a more difficult task. On the other side, the results in Figure 8 (b) show the performance of H-OWAN is not sensitive with the change of rank of T1CL.

4.3 E3: IR under Five Types of Distortion

Below, we use numerical experiments to demonstrate that H-OWAN with higher orders has promising performance on more challenging tasks.

Experiment setting Compared to E1, we consider additional two types of distortion, *i.e.* raindrop and salt-and-pepper noise. The dataset adopted in this experiment is from Raindrop [16], where we cropped the original images into 123,968, 5,568 and 25,280 patches for training, validation and test, respectively. Apart from CP decomposition, we also represent the tensor kernel in T1CL by TT and TR given in Sec. 3. Other setting for both the data and networks are same to ones in E1.

Experimental results Figure 6 shows the performance constellation including many variants of H-OWAN. In the figure, the number following specific TN decomposition like "CP3"

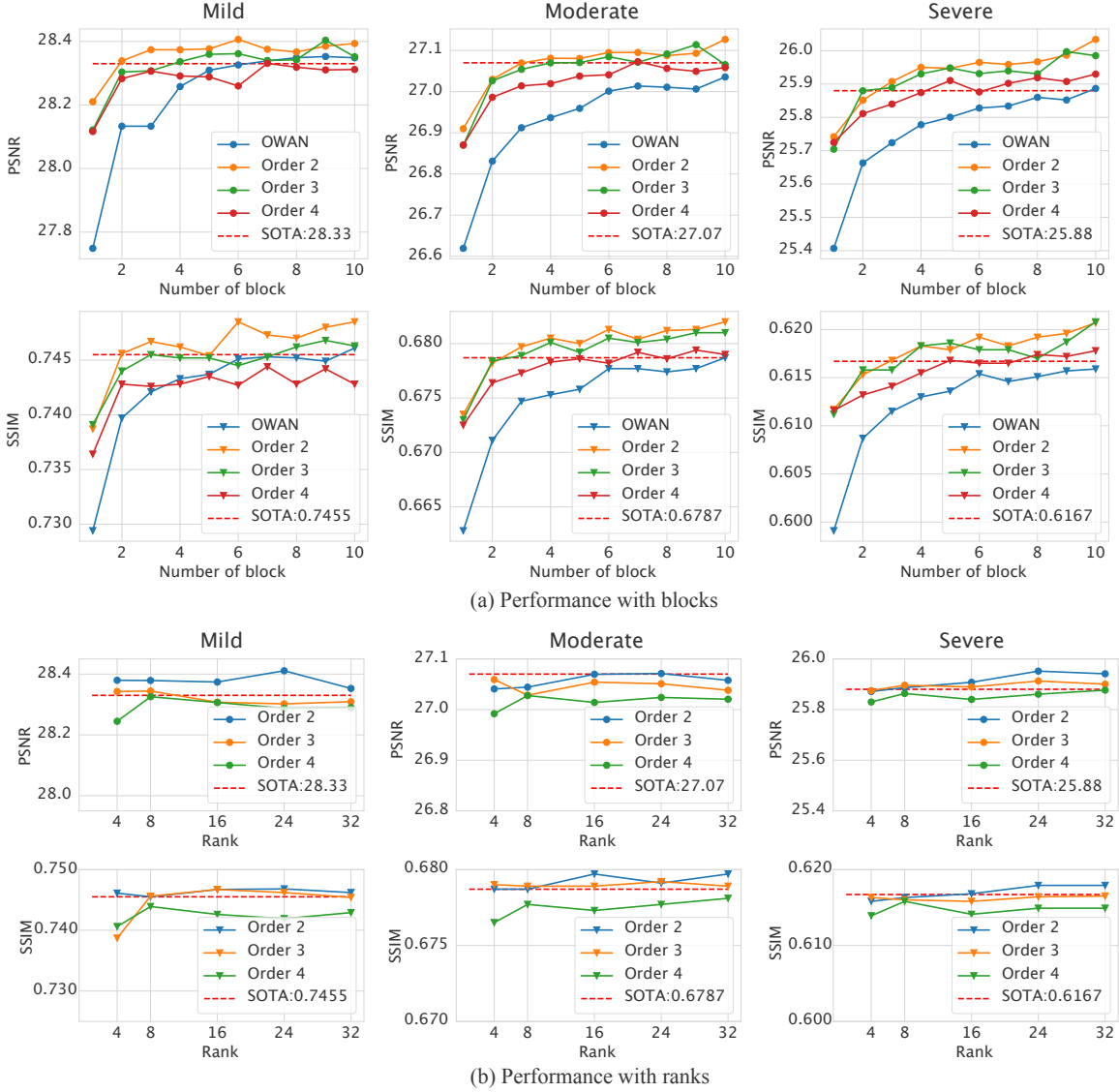


Figure 8: The results of PSNR and SSIM with different orders, number of blocks and rank. In (a) we fix the rank equaling 16, while in (b) we fix the number of blocks equaling 3 for illustration. The red dashed line shows the result by OWAN.

and “TR4” denotes the order used in the network, and the keywords “(un)share” represents whether assuming the symmetric structure of the kernels in T1CLs. As shown in Figure 6, H-OWAN with 3-order tensor ring format obtains the SOTA performance. More interestingly, with increasing the strength of the distortion, *i.e.* from mild to severe level, more points appear on the right-top counter of this figure. It can be inferred that the H-OWANs with higher orders and sophisticated TN decomposition would have more promising performance to handle more challenging restoration tasks.

5 Conclusion

Compared to the original OWAN, its high-order extension, *a.k.a.* H-OWAN, achieves the state-of-the-art performance on the multi-distorted image restoration task (see Table 5). Furthermore, the performance improvement is always kept under various hyper-parameters and configurations (see Figure 8). We therefore argue that the proposed tensor 1×1 convolutional layer (T1CL) not only can effectively alleviate the heterogeneity of features by multiple operations (see Figure 2), but also provides powerful representation ability due to the additional non-linearity by tensor product (see Figure 6).

References

- [1] Hedi Ben-Younes, Rémi Cadene, Matthieu Cord, and Nicolas Thome. Mutan: Multimodal tucker fusion for visual question answering. In *Proceedings of the IEEE international conference on computer vision*, pages 2612–2620, 2017.
- [2] Thomas Gerstner and Michael Griebel. Dimension-adaptive tensor-product quadrature. *Computing*, 71(1):65–87, 2003.
- [3] Ming Hou, Jiajia Tang, Jianhai Zhang, Wanzeng Kong, and Qibin Zhao. Deep multimodal multilinear fusion with high-order polynomial pooling. In *Advances in Neural Information Processing Systems*, pages 12113–12122, 2019.
- [4] Diederik P Kingma and Jimmy Ba. Adam: A method for stochastic optimization. *arXiv preprint arXiv:1412.6980*, 2014.
- [5] Ogun Kirmemis, Gonca Bakar, and A Murat Tekalp. Learned compression artifact removal by deep residual networks. In *CVPR Workshops*, pages 2602–2605, 2018.
- [6] Tamara G Kolda and Brett W Bader. Tensor decompositions and applications. *SIAM review*, 51(3):455–500, 2009.
- [7] Yudong Liang, Ze Yang, Kai Zhang, Yihui He, Jinjun Wang, and Nanning Zheng. Single image super-resolution via a lightweight residual convolutional neural network. *arXiv preprint arXiv:1703.08173*, 2017.
- [8] Huangxing Lin, Xueyang Fu, Changxing Jing, Xinghao Ding, and Yue Huang. A²net: Adjacent aggregation networks for image raindrop removal. *arXiv preprint arXiv:1811.09780*, 2018.
- [9] Wei Liu, Dragomir Anguelov, Dumitru Erhan, Christian Szegedy, Scott Reed, Cheng-Yang Fu, and Alexander C Berg. Ssd: Single shot multibox detector. In *European conference on computer vision*, pages 21–37. Springer, 2016.
- [10] Zhun Liu, Ying Shen, Varun Bharadhwaj Lakshminarasimhan, Paul Pu Liang, Amir Zadeh, and Louis-Philippe Morency. Efficient low-rank multimodal fusion with modality-specific factors. *arXiv preprint arXiv:1806.00064*, 2018.
- [11] Ilya Loshchilov and Frank Hutter. Sgdr: Stochastic gradient descent with warm restarts. *arXiv preprint arXiv:1608.03983*, 2016.
- [12] Alexander Novikov, Mikhail Trofimov, and Ivan Oseledets. Exponential machines. *arXiv preprint arXiv:1605.03795*, 2016.
- [13] Ivan V Oseledets. Tensor-train decomposition. *SIAM Journal on Scientific Computing*, 33(5):2295–2317, 2011.
- [14] Jinshan Pan, Deqing Sun, Hanspeter Pfister, and Ming-Hsuan Yang. Blind image deblurring using dark channel prior. In *Proceedings of the IEEE Conference on Computer Vision and Pattern Recognition*, pages 1628–1636, 2016.
- [15] Xingang Pan, Ping Luo, Jianping Shi, and Xiaoou Tang. Two at once: Enhancing learning and generalization capacities via ibn-net. In *Proceedings of the European Conference on Computer Vision (ECCV)*, pages 464–479, 2018.
- [16] Rui Qian, Robby T Tan, Wenhan Yang, Jiajun Su, and Jiaying Liu. Attentive generative adversarial network for raindrop removal from a single image. In *Proceedings of the IEEE Conference on Computer Vision and Pattern Recognition*, pages 2482–2491, 2018.
- [17] Sukhwinder Singh, Robert NC Pfeifer, and Guifré Vidal. Tensor network decompositions in the presence of a global symmetry. *Physical Review A*, 82(5):050301, 2010.
- [18] Masanori Suganuma, Xing Liu, and Takayuki Okatani. Attention-based adaptive selection of operations for image restoration in the presence of unknown combined distortions. In *Proceedings of the IEEE Conference on Computer Vision and Pattern Recognition*, pages 9039–9048, 2019.
- [19] Ying Tai, Jian Yang, Xiaoming Liu, and Chunyan Xu. Memnet: A persistent memory network for image restoration. In *Proceedings of the IEEE international conference on computer vision*, pages 4539–4547, 2017.
- [20] Xin Tao, Hongyun Gao, Xiaoyong Shen, Jue Wang, and Jiaya Jia. Scale-recurrent network for deep image deblurring. In *Proceedings of the IEEE Conference on Computer Vision and Pattern Recognition*, pages 8174–8182, 2018.
- [21] Ke Yu, Chao Dong, Liang Lin, and Chen Change Loy. Crafting a toolchain for image restoration by deep reinforcement learning. In *Proceedings of the IEEE conference on computer vision and pattern recognition*, pages 2443–2452, 2018.
- [22] Ke Yu, Xintao Wang, Chao Dong, Xiaoou Tang, and Chen Change Loy. Path-restore: Learning network path selection for image restoration. *arXiv preprint arXiv:1904.10343*, 2019.
- [23] Rose Yu, Stephan Zheng, Anima Anandkumar, and Yisong Yue. Long-term forecasting using higher order tensor rnns. *arXiv preprint arXiv:1711.00073*, 2017.
- [24] Kai Zhang, Wangmeng Zuo, Yunjin Chen, Deyu Meng, and Lei Zhang. Beyond a gaussian denoiser: Residual learning of deep cnn for image denoising. *IEEE Transactions on Image Processing*, 26(7):3142–3155, 2017.
- [25] Qibin Zhao, Guoxu Zhou, Shengli Xie, Liqing Zhang, and Andrzej Cichocki. Tensor ring decomposition. *arXiv preprint arXiv:1606.05535*, 2016.